Scientific Research

Usefulness of the SNR Using the Subtraction Method and Image Visibility Using the Howlett Chart Method in X-Ray Fluoroscopic System

Sadamitsu Nishihara[1], Yuki Yamashita[2,3], Naoki Kawai[2,4], Hideki Otsuka[1]

[1]Subdivision of Biomedical Information Sciences, Institute of Health Biosciences, University of Tokushima Graduate School, Tokushima, Japan
[2]Department of Radiological Technology, Tokushima University School of Health Sciences, Tokushima, Japan
[3]Department of Radiological Technology, University of Miyazaki Hospital, Miyazaki, Japan
[4]Department of Radiology, Kansai Electric Power Hospital, Osaka, Japan
Email: nishihara.sadamitsu@tokushima-u.ac.jp

Abstract

X-ray fluoroscopy has been used not only for diagnoses but also for treatment, as in interventional radiology. The aim of this study is to assess the usefulness of the signal-to-noise ratio (SNR) using the subtraction method, which is used in the quality assurance/quality control (QA/QC) of magnetic resonance imaging (MRI) equipment, and image visibility using the Howlett chart method in the fluoroscopic examination. The fluoroscopy unit has a detector with an image intensifier and a color liquid crystal display. A 2620 dosimeter and an ionization chamber were selected for the dose measurement. Fluoroscopic images for visual and physical evaluations were collected as dynamic data. The skin surface absorbed dose rates for each tube current were measured using a dosimeter. The SNR using the subtraction method and image visibility using the Howlett chart method were examined. The results from both indicate that as the SNR improves, visual evaluation increases, but the rate of increase gradually saturates. Therefore, physical and visual evaluations are possible with the SNR using the subtraction method and the image visibility using the Howlett chart method.

Keywords

1. Introduction

X-ray fluoroscopy has been used not only for diagnoses but also for treatment, as in interventional radiology. The dose distribution in the irradiation field of the image intensifier (II) is non-uniform, and an image obtained by the II includes distortion. Therefore, it is necessary to solve this problem to evaluate an image.

The following two methods were used to solve this problem in both physical and visual evaluations. For evaluating dynamic-image frames, such as those of fluoroscopic images, basic and physical measurements such as the signal-to-noise ratio (SNR) or contrast-to-noise ratio were used [1]-[4]. This study used the difference method, which is adopted for quality assurance/quality control (QA/QC) evaluation of magnetic resonance imaging (MRI) and for SNR measurements [5]. A merit of this method is that the non-uniformity of the image and the heel effect can be removed. On the other hand, some measurements are used to visually evaluate an image. For example, there is the instantaneous detectability or detection rate of the alternative forced-choice method and low-contrast object detectability using a contrast-detail phantom [2] [4] [6] [7]. The size of the phantom affects the detectability in visual evaluations. A few studies have estimated visibility using the Howlett chart in fluoroscopic imaging [8]. The Howlett chart is small, its influence on the visibility that depends on the non-uniformity of the II is small. Moreover, it is able to discuss a change in visibility by the difference in spatial frequency.

The aim of this study is to assess the usefulness of the SNR using the subtraction method and image visibility using the Howlett chart method in the fluoroscopic examination.

2. Methods and Materials

2.1. Equipment

The detector for fluoroscopy used in this study was an II (RTP12302J-G9; Toshiba Inc., Tokyo, Japan), and the detector unit was combined with a color liquid crystal display (CDL2013-1A/R; Toshiba Inc., Tokyo, Japan). The phantom for visual evaluation was the Howlett chart (l-90-P; Nikko Fines industries, Co., LTD., Tokyo, Japan). The Howlett chart comprises nine sets in a 3 * 3 matrix with thirteen signals, *i.e.*, different-sized circles. The inside diameter of a cycle ranges from 0.125 to 1.0 mm (spatial frequency: 0.5 - 4.0 cycles/mm), and the ratio of the outside to inside diameter is 3:1. **Figure 1** shows an example of the Howlett chart image during exposure in a fluoroscopic system.

A 2620 dosimeter (NE Technology LTD., Beenham, UK) and an ionization chamber (DC300 TNC/168; IBA/scanditronix Wellhofer, Schwarzenbruck, Germany) were selected for the dose measurement.

2.2. Dynamic Image Data

The fluoroscopic images for visual and physical evaluations were collected as dynamic data. **Figure 2** shows the schematic diagram of this experiment. An 8-cm-thick polymethyl methacrylate (PMMA) plate was added as a filter for X-ray attenuation. The distance from the focal spot of the X-ray tube to the bed was 110 cm, and the Howlett chart was located at the center of the irradiation field. Exposure conditions were as follows: tube voltage, 60 kV; tube current, 0.5, 1, 2, 3, and 4 mA; fluoroscopic time, 10 s; irradiation field, 6 inches (about 15 cm in diameter); and frame rate, 15 frames/s.

Dynamic image data were collected at the fixed frame rate (15 frames/s) and fluoroscopic time (10 s) for each tube current. Moreover, the frame rate was 7.5 frames/s only when the tube current was 4 mA. The width and level of the window were set to be constant in all data sets so that the brightness that was measured by the luminance meter was 47 ± 1 (cd/m^2).

2.3. Skin Surface Absorbed Dose Rate (SSADR)

The SSADRs in each tube current were measured by a dosimeter. The ionization chamber was set up to measure an exposure at a height of 20 cm from the bed, and at the center of the irradiation field, the dosimeter was positioned at a height of 20 cm because the thickness of the human body is approximately 20 cm. The exposure for each tube current was measured under the condition of 10 s in fluoroscopic time. This study design was to obtain three measurements for each tube current on three different days (nine measurements in total) and calculate the mean of the exposures. The exposures were converted into dose rates per minute by multiplying the doses by a temperature–pressure correction factor, backscatter factor, and absorbed dose conversion factor.
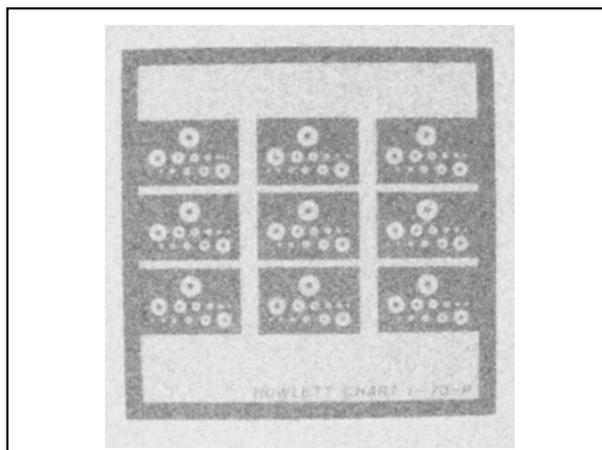
Figure 1. The static image of a Howlett chart during exposure in a fluoroscopic system (Tube voltage: 60 kV, Tube current: 4 mA).
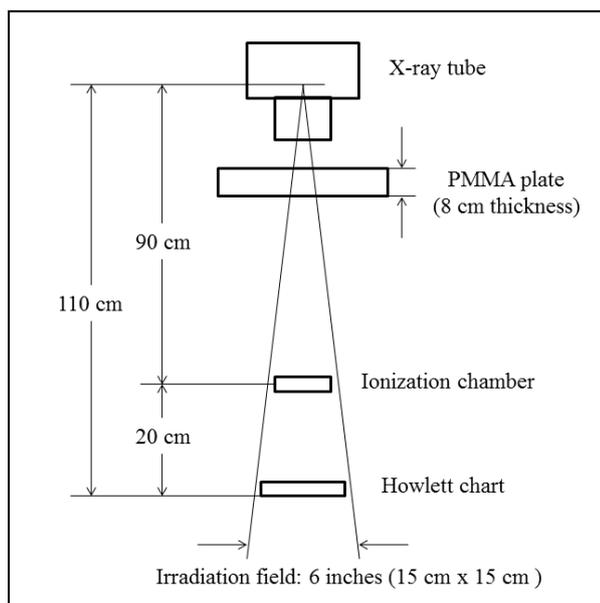

Figure 2. Schematic diagram of the experiment.

2.4. Physical Image Property

2.4.1. Reference Image

The SNR was adopted as a physical image property. The standard image was selected in each tube current out of a dynamic image series to calculate the SNR using a subtraction method [5]. There were 150 static images (15 [frames/s] * 10 [s]) in one dynamic series, and fifteen images were selected at random from each series. The normality of the observation results for the fifteen images was examined and an image that was closest to the average was selected. A selected image was determined for the entire dynamic series because normality was obtained in all series in this experiment. Therefore, the selected image was used as the standard image.

2.4.2. Calculation of SNR

The matrix size of the dynamic image data was 1024 * 1024. First, the average value was measured in two regions of interest (ROIs, size: 25 pixels * 25 pixels), which were located on the standard image (**Figure 3(a)**) using ImageJ software (NIH: ver.1.1.4.3.67). Second, the subtraction image, in which the standard image was

(a)   (b)
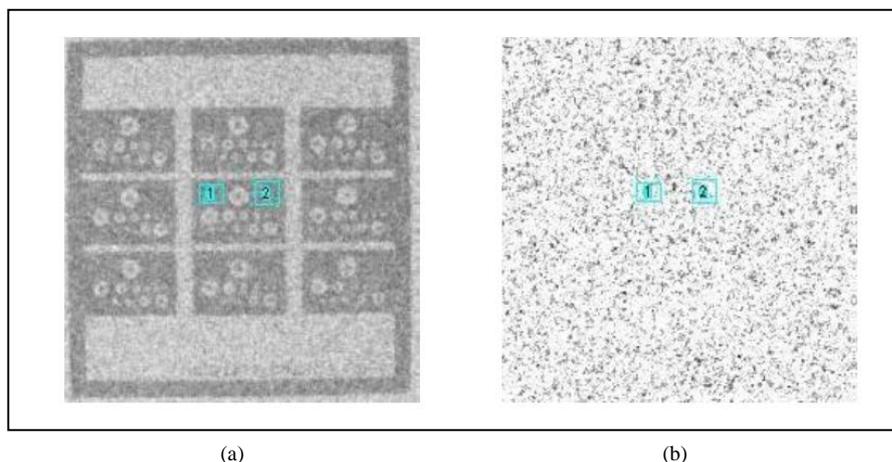
Figure 3. Two regions of interest on the static image: (a) For signal data; (b) For noise data.

subtracted from each dynamic image, was obtained, and the standard deviation (SD) was measured in the same ROIs, which were located on the subtraction image (**Figure 3(b)**). Third, 149 SDs were measured from 149 subtraction images (150 images—one standard image), and 149 SNRs were calculated using these SDs and the average signal value. Finally, the average of 149 SNRs was the SNR for the dynamic image series of each tube current.

2.5. Observer Performance

2.5.1. Samples
Eleven observation series were arranged as follows: 1) Dynamic image series: 0.5, 1, 2, 3, and 4 mA (15 frames/s) and 4 mA (7.5 frames/s); and 2) Static image series: 0.5, 1, 2, 3, and 4 mA. Moreover, the standard image that was used for physical evaluation of a static image was used.

2.5.2. Informed Consent
Subjects comprised 19 students in the School of Health Sciences, the University of Tokushima. This study was approved by the ethics committee of the University of Tokushima Hospital, and the subjects gave written informed consent prior to participation.

2.5.3. Observer Study
The viewing distance was 75 cm. The observer's forehead and chin were fixed so that he/she could always make an observation at a fixed spot. Experiments were performed in a darkened room. The observer selected the smallest recognizable black circle (signal) out of the black circles displayed on each plate of the Howlett chart. The decision criterion was whether the signal can be recognized as an exact circle. Signals were numbered in the order of the largest to the smallest, and the observer was instructed to state the number assigned to the smallest signal. In the case when the observer could only see a signal larger than the smallest one, he/she was instructed to state the number assigned to the smallest visible signal. Because the order of observing data sets is the same in the present experiment, the first three data sets (dynamic images: 3 mA; static images: 2 mA; and frame rate: 7.5 frames/s) were observed again at the end, and the results of these last three trials were used.

3. Results

3.1. SSADR and SNR Using the Subtraction Method

The graph showing the result of the physical evaluation: the SNRs obtained for the SSADR are shown in **Figure 4**. The SNR increase with increasing SSADR, and the curving rate of the graph gradually becomes gentler. The relationship of both can be expressed by a power approximation. There are two conditions for improving the SNR: increase the signal (average value) and decrease the noise (SD). For the present experiment, the signals were almost the same at any tube current. However, noise decreased as the tube current increased, and this result
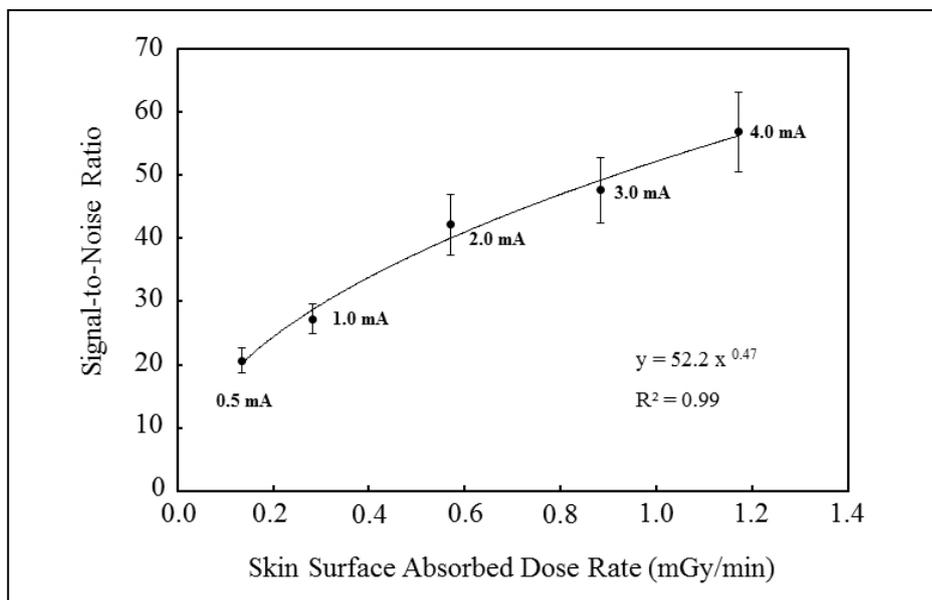
Figure 4. Signal-to-noise ratio for skin surface absorbed dose rate.

showed a tendency to become diminished. In summary, the present change in the SNR was affected by the change in noise, and therefore, improving the SNR by increasing the dose rate means reducing the noise.

3.2. Visibilities by Howlett Chart Method

The results of the observation performance are shown in **Figure 5**. The horizontal axis of the graph represents spatial frequency, and the vertical axis, visibility. Visibility indicates the rate of detection for each spatial frequency. As shown in **Figure 5**, the overall visibility of dynamic images is the lowest for 0.5 mA and the highest for 4 mA. There was almost the same trend in the range of 1 to 4 mA, but the visibility began to decline at around 1.0 cycle/mm, and there was almost no visibility at around 2.0 cycles/mm.

A graph of the area of visibility calculated for each SSADR is shown in **Figure 6**. Using the results from 19 observers, the area of visibility for each spatial frequency range was calculated. The results of the normality test for the conditions of each data set showed that almost all of them had normality. Therefore, the average value was used as the reference index for visual evaluation. As shown in **Figure 6**, as the SSADR increases, visual evaluation increases, but the rate of increase gradually saturates. This is probably because of the decrease in noise due to a smaller increase in the SSADR, so that the visibility of the high spatial-frequency signal did not improve, resulting in a smaller change in the visual evaluation.

4. Discussion

The relationship between the exposure quanta and the input SNR can be defined using Equation (1) [9].

$$\mathrm{SNR_{input}} = \sqrt{\mathrm{exposure\ quanta}} \tag{1}$$

When the analog-to-digital (AD) converter of our fluoroscopic system is assumed to be a linear type, the SNR is described by Equation (2).

$$\mathrm{SNR} \propto a \times \sqrt{\mathrm{SSADR}} = a \times \mathrm{SSADR}^{0.5} \tag{2}$$

Here *a* is constant. The equation of the approximate curve is as follows.

$$\mathrm{SNR} = 52.2 \times \mathrm{SSADR}^{0.47} \tag{3}$$

Therefore, it is considered that the results of this study do not have a contradiction.

The correlation between these two evaluations, based on the results of the physical evaluation (**Figure 4**) and visual evaluation (**Figure 6**), is shown in **Figure 7**. As shown in **Figure 7**, the SNR improves, visual evaluation
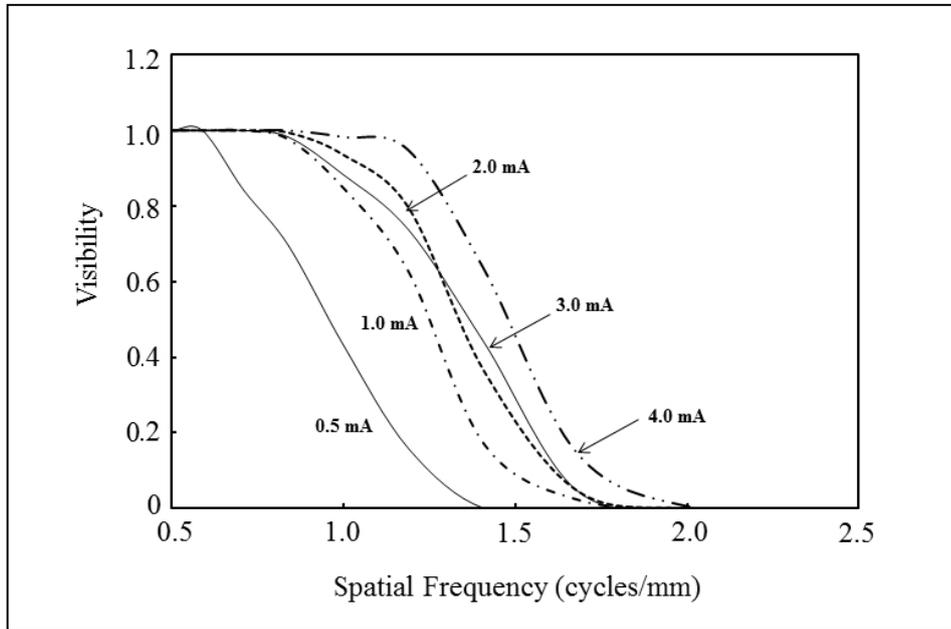
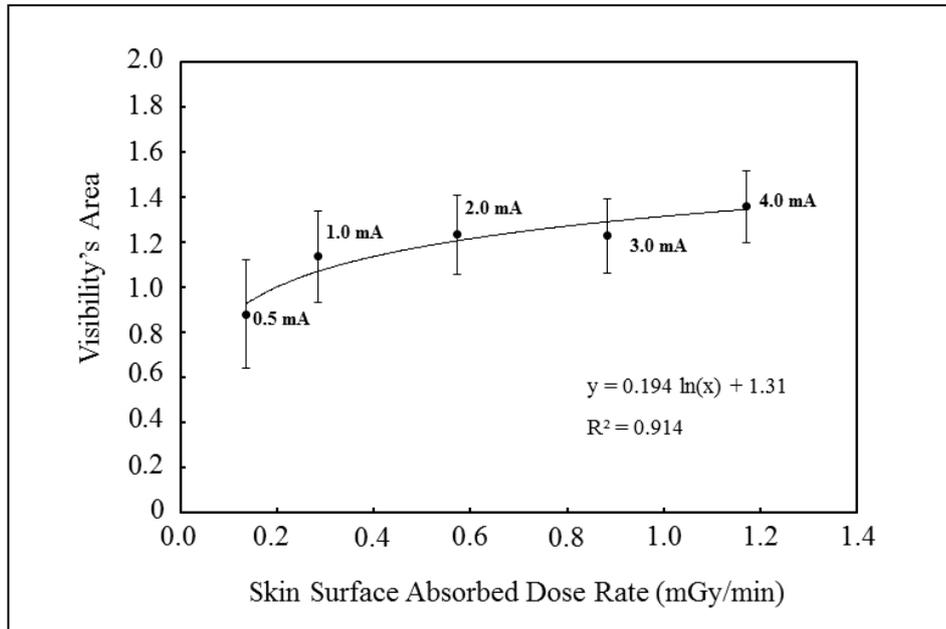**Figure 5.** The results of the present observation experiment.

Figure 6. Area of visibility versus skin surface absorbed dose rate.

increases, but the rate of increase gradually saturates. The relationship between image quality and diagnostic accuracy is unclear, *i.e.*, whether improving the quality of physical images always improves the diagnostic accuracy, and this does not contradict our results [7] [10].

The spot on the right end (◊) in **Figure 7** was obtained at 4 mA and 7.5 frames/s. The SNR of dynamic images obtained under the same conditions was higher than that of images obtained at 4 mA and 15 frames/s, but the former was found to be lower than the latter as a result of the visual evaluation. This means that an increase in the number of frames reproduced may improve the visual evaluation more than the SNR.

The reason for using the Howlett chart and not a Burger Phantom was because signal values at the center and the periphery of images detected by the II differ [8]. Since the fluorescent screen of the II is convex, the angles
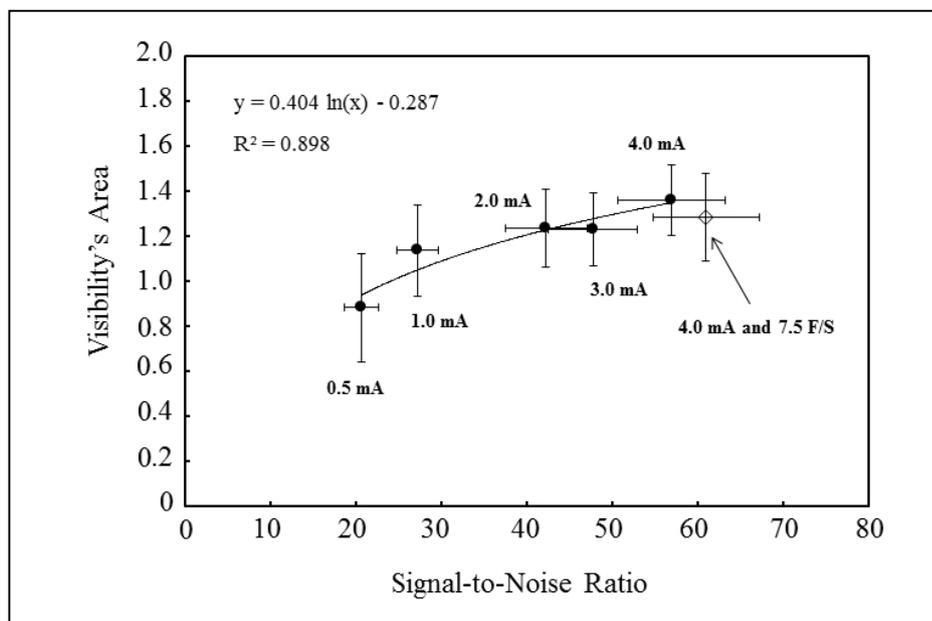
Figure 7. Relationship between signal-to-noise ratio and visibility.

of the detector plane to the X-ray at the center and the periphery are so different that the angle of the plane to the X-ray at the center is perpendicular while that at the periphery is diagonal. Therefore, the density of the X-ray detected becomes coarser as the detector position moves away from the center. This means that the signal value decreases toward the periphery of the image. A Burger Phantom is large, so it affects the signal value at any other spot than at the center of the image. Therefore, we used a smaller-sized Howlett chart. Moreover, we also set up the ROIs at two spots close to the center of the image for measurement of the SNR.

5. Conclusion

The usefulness of the SNR using the subtraction method, which is used in the QA/QC of MRI equipment, and the image visibility using the Howlett chart method in the fluoroscopic examination was discussed. The relationship between SNR and SSADR can be indicated by a power approximation, and as the SSADR increases, visibility increases; however, the rate of increase gradually saturates. Similar results have been found in a few other studies. Therefore, both physical and visual evaluations are possible with the SNR using the subtraction method and the image visibility using the Howlett chart method.

References

[1]   Yamao, Y., Yamakado, K., Takaki, H., Yamada, T., Murashima, S., Uraki, J., Kodama, H., Nagasawa, N. and Takeda, K. (2010) Optimal Scan Parameters for CT Fluoroscopy in Lung Interventional Radiologic Procedures: Relationship between Radiation Dose and Image Quality. *Radiology*, **255**, 233-241. http://dx.doi.org/10.1148/radiol.09090733

[2]   Honda, M., Kitadani, S. and Ishii, H. (2007) Observer Performance for a Linear Pattern with Different Frequency Characteristics of Background Random Noise. *Proceeding of the* 2*nd International Conference on Complex Medical Engineering-CME*, Beijing, 23-27 May 2007, 1471-1476.

[3]   Tapiovaara, M.J. (1993) SNR and Noise Measurements for Medical Imaging: II. Application to Fluoroscopic X-Ray Equipment. *Physics in Medicine and Biology*, **38**, 1761-1788. http://dx.doi.org/10.1088/0031-9155/38/12/006

[4]   Tapiovaara, M.J. (1997) Efficiency of Low-Contrast Detail Detectability in Fluoroscopic Imaging. *Medical Physics*, **24**, 655-664. http://dx.doi.org/10.1118/1.598076

[5]   Ogura, A., Miyai, A., Maeda, F., Fukutake, H. and Kikumoto, R. (2003) Accuracy of Signal-to-Noise Ratio Measurement Method for Magnetic Resonance Image. *Nihon Hoshasen Gijutsu Gakkai Zasshi*, **59**, 508-513. (in Japanese)

[6]   Aufrichig, R., Xue, P., Thomas, C.W., Gilmore, G.C. and Wilson, D.L. (1994) Perceptual Comparison of Pulsed and Continuous Fluoroscopy. *Medical Physics*, **21**, 245-256. http://dx.doi.org/10.1118/1.597285

[7] Tapiovaara, M.J. and Sandborg, M. (2004) How Should Low-Contrast Detail Detectability be Measured in Fluoroscopy? *Medical Physics*, **31**, 2564-2576. http://dx.doi.org/10.1118/1.1779357

[8] Yoshizawa, H. (2001) Image Quality Evaluation of Digital Radiography (DR) System Using Howlett Chart. *The Journal of Tokyo Academy of Health Sciences*, **3**, 257-261. (in Japanese)

[9] Dainty, J.C. and Shaw, R. (1974) Image Science. Academic Press Inc., New York.

[10] US Department of Health and Human Services, Bureau of Radiological Health Report (1982) MTF's and Wiener Spectra of Radiographic Screen-Film Systems. HHS Publication FDA 82-8187, Rockville.